Elastoplastic analysis of frames composed of softening materials by restricted basis linear programming

M.R. Mahini [a], H. Moharrami [b,*], G. Cocchetti [c]

[a] Department of Civil Engineering, Persian Gulf University, Boushehr, Iran
[b] Department of Civil and Environmental Engineering, Tarbiat Modares University, Tehran, Iran
[c] Department of Structural Engineering, Technical University (Politecnico) of Milan, Piazza L. da Vinci, 32-20133 Milan, Italy

Article history:
Received 13 December 2012
Accepted 14 August 2013
Available online 3 October 2013

1. Introduction

Elasto-plastic analysis of frames with softening material has been the subject of research and interest for many researchers during last decades (see e.g., [1,2]). The necessity of more realistic solutions for frames subject to increasing lateral loads, makes this topic a well-known and still growing area among other engineering research topics [3–5]. To this end some simplifying assumptions are found to be practical and efficient. Among them are: lumping plasticity in some pre-selected sections, using piecewise-linear yield surfaces and ignoring path dependency and possible local unloading (i.e., "holonomic" behavior) over each load step. Beside these simplifying assumptions, optimization is found to be a very powerful and versatile computational tool for the direct analysis of nonlinear problems [6]. A brief review of such approaches in the field follows.

Linear Programming (LP) has long been recognized as a suitable tool for limit state analysis of structures. In the classical limit analysis, when loads are applied to a framed structure and are assumed to increase proportionally, on the basis of the well-known lower- and upper-bound theorems the limit load and the collapse configuration can be computed as a solution to a linear mathematical programming problem [7,8]. This approach is known to be a milestone in the history of structural mechanics and still is a common approach for engineers in a variety of practical problems, but also a developing subject in the literature (see [2,9]).

Maier [10,11] proposed the use of mathematical programming in elasto-plastic analysis of structures, for which the nonlinear holonomic response is sought as solution to a Quadratic Programming (QP) problem. Later on, the method was extended to consider the interaction of axial force and bending moment by adopting a piece-wise linear yield surface [12]. In order to increase the efficiency of the solution procedure, in some later researches the QP formulation was replaced by a Linear Complementarity Problem (LCP), [13], and by a Restricted Basis Linear Programming (RBLP) [14]. This approach was also improved and generalized to shakedown and nonlinear dynamic analyses [15,16]. Cocchetti and Maier implemented the aforementioned approach in the analysis of softening frames [17]. They proposed two procedures, namely a step-by-step method (SBSM) and a stepwise holonomic/fully holonomic analysis, and discussed them in detail. In both solution schemes, the load multiplier is considered as the objective function to be maximized and the structural response is sought as the solution(s) to an LCP. Load factor maximization has also been employed by Lógó and Taylor in developing the so called "Extremum Principle" [18] and implemented by Kaliszky and Lógó in analysis of truss structures [19]. Clearly, in the case of softening negative load increments are expected and, as a consequence, the load maximization principle fails. This problem was discussed in [17], and in such a case, a new solution to LCP for negative load increments was proposed as a remedy. Another holonomic approach was proposed by Tangaramvong and Tin-Loi to deal with structures governed by piecewise linear softening models [20]. This method employs a penalty approach to solve the nonlinear optimization problem, but the penalty parameter that enforces complementar-

* Corresponding author. Tel./fax: +98 21 82883324.
E-mail address: hamid@modares.ac.ir (H. Moharrami).

ity has to be carefully selected to prevent numerical instabilities. Some recommendations are given on the selection of the penalty coefficient, but it seems that this parameter and its updating schedule do not follow any clear rule.

Recently, Mahini et al. [21] proposed a new dissipated energy maximization (DEM) approach in which the solution to the incremental LCP (in terms of plastic multipliers) is obtained as the solution to an LP problem by exploiting a plastic work criterion. This approach has shown to have distinct ability in solving frames composed of elastic-perfectly-plastic materials. In this approach, the incremental LP problem is formulated in terms of all problem variables (i.e., load and plastic multipliers), just like it is done in other holonomic formulations; but as a result of additional restrictions applied to the vector of basic variables, "exactness" and "stability" features of a step-by-step method are preserved. This approach is characterized by a non-holonomic nature and it can perform any required local unloading: the resulting refreshed Simplex table always represents the updated configuration and, in this sense, the loading process can continue without any extra computational effort.

However the dissipated power has been frequently employed as an internal variable for hardening/softening constitutive model construction, (see e.g., [22]), in DEM approach maximization of the dissipated power is used as a tool for recognizing the correct path of plastic deformations in the space of plastic multipliers.

In this paper, the DEM solution strategy is extended to the softening frames and is shown to be capable of tracing the exact response by detecting any elastic unloading and any equilibrium bifurcation. For this purpose, the theoretical aspects of the method are discussed in Section 2. The piecewise linear softening model, with interacting planes, for a typical frame section (or "joint") is developed in Section 2.1. The problem formulation is illustrated in Section 2.2. Some terms and definitions regarding the solution algorithm are given in Section 2.3. The solution to the incremental LP problem is described in Section 3. Afterwards, some numerical examples are discussed in Section 4 to demonstrate the robustness of the proposed algorithm and show its capabilities. Finally, Section 5 is devoted to discussions and final conclusions.

2. Theoretical aspects

As stated above, the current version of DEM has been proposed for frames with elastic-perfectly-plastic behavior. In order to modify the algorithm for the softening frame analyses, the formulation is updated and some modifications are discussed in the following.

2.1. Piecewise-linear softening model for the joint

Piecewise-linearized constitutive models are reasonable assumptions and effective formulation tools in nonlinear analysis of framed structures (see e.g., [23,24]). In this study, a 6-mode piecewise-linear yield surface is considered and an isotropic softening rule is adopted to describe the evolution of the yield locus (see Fig. 1a).

For the joint s, a PWL yield surface with isotropic softening can be given the following mathematical description:

$$\mathrm{Y}_s = \mathbf{\Phi}_s^{\mathrm{T}} \mathrm{f}_s - \alpha_s \leqslant 0, \tag{1}$$

where, f_s is the vector of generalized stresses (axial force, N_s, and bending moment, M_s) acting on the cross-section s:

$$\mathrm{f}_s = \begin{Bmatrix} N_s \\ M_s \end{Bmatrix}. \tag{2}$$

Matrix $\mathbf{\Phi}_s$ contains the normal vectors of the yield planes (normalized w.r.t. the corresponding plastic capacities N_p and M_p); for the 6-mode PWL yield locus shown in Fig. 1a, ($m = 6$) it assumes the following form:

$$\mathbf{\Phi}_s = \begin{bmatrix} \frac{\varphi^s_{N1}}{N_\mathrm{p}} & \frac{\varphi^s_{N2}}{N_\mathrm{p}} & \frac{\varphi^s_{N3}}{N_\mathrm{p}} & \frac{\varphi^s_{N4}}{N_\mathrm{p}} & \frac{\varphi^s_{N5}}{N_\mathrm{p}} & \frac{\varphi^s_{N6}}{N_\mathrm{p}} \\ \frac{\varphi^s_{M1}}{M_\mathrm{p}} & \frac{\varphi^s_{M2}}{M_\mathrm{p}} & \frac{\varphi^s_{M3}}{M_\mathrm{p}} & \frac{\varphi^s_{M4}}{M_\mathrm{p}} & \frac{\varphi^s_{M5}}{M_\mathrm{p}} & \frac{\varphi^s_{M6}}{M_\mathrm{p}} \end{bmatrix}_{2\times m}. \tag{3}$$

In the above formula, indices 1–6 refer to the yield planes and ϕ_{ij} is the partial derivative of the jth yield plane with respect to ith generalized stress.

Each entry α^s_j of vector α_s is related to the distance of the jth yield plane from the origin, so that α_s determines the size/shape of yield surface at any loading instance. According to the isotropic softening rule, it is convenient to relate the size change of the yield locus to an internal scalar variable describing the irreversible evolution. To this end, a generalized equivalent plastic strain, ε^s_p, is defined as a linear combination of plastic multipliers, x_s (which is a $m \times 1$ vector and for the selected 6-mode piecewise-linear yield surface $m = 6$), of the joint model as follows:

$$\varepsilon^s_\mathrm{p} = \overline{\mathbf{Q}}_s \mathrm{x}_s. \tag{4}$$

$\overline{\mathbf{Q}}_\mathbf{s}$ is a row-vector collecting the magnitudes of the yield locus normal vectors:

$$\overline{\mathbf{Q}}_\mathbf{s} = [\, n^1_s \quad n^2_s \quad n^3_s \quad n^4_s \quad n^5_s \quad n^6_s \,]_{1\times m}. \tag{5}$$

Plastic behavior of softening frame joints is usually simplified in three general phases: initial yielding phase, softening phase and ultimate strength phase. In the first and last phases, the material is assumed to behave fully plastic; instead, in the second phase the strength decreases due to softening. Fig. 1c shows such a 3-phase softening rule. Parameters ε^p_{s1} and ε^p_{s2} are the equivalent plastic strain limits at which the softening branch and final limit phase begin, respectively. The evolution law depicted in Fig. 1c can be mathematically described by three (non-negative) plastic multipliers ($\bar{x}^0_s, \bar{x}^1_s$ and $\bar{x}^2_s$) and the following relationships:

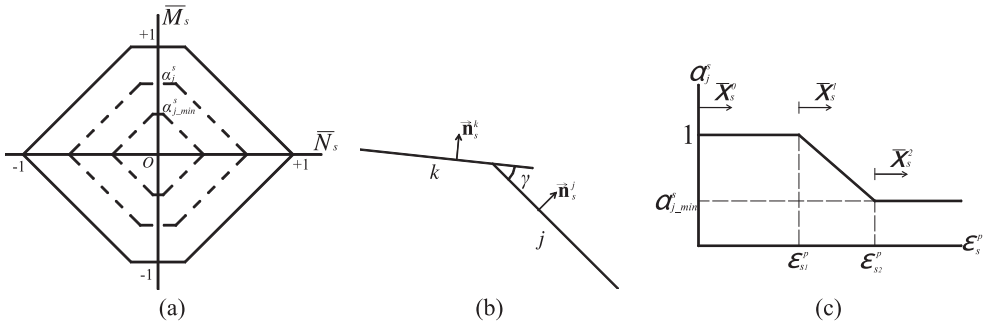

Fig. 1. Constitutive softening model in terms of normalized internal actions: (a) typical 6-mode piecewise linear yield surface and its evolution with isotropic softening, (b) intersection of two adjacent yield planes (j and k) and their corresponding normal vectors, and (c) three phase softening rule.

$$\begin{aligned}&\bar{x}_s^0 \leqslant \varepsilon_{s1}^{p},\\&\bar{x}_s^1 \leqslant \varepsilon_{s2}^{p} - \varepsilon_{s1}^{p},\\&\bar{x}_s^0 + \bar{x}_s^1 + \bar{x}_s^2 = \varepsilon_s^{p}.\end{aligned} \tag{6}$$

By solving the last equation for the softening variable $\bar{x}_s^0$ and replacing the result into the first inequality, the constraints will be reduced only to inequalities. After these simplifications, the above softening constraints can be given the following compact matrix notation:

$$Z_s = \mathbf{Q}_s x_s + \mathbf{W}_s \bar{x}_s - C_s \leqslant \{0\} \tag{7}$$

in which:

$$\begin{aligned}\mathbf{Q}_s &= \begin{bmatrix}\overline{\mathbf{Q}}_s\\ \mathbf{0}\end{bmatrix}_{2\times m},\\ \mathbf{W}_s &= \begin{bmatrix}-1 & -1\\ 1 & 0\end{bmatrix}_{2\times 2},\\ C_s &= \begin{Bmatrix}\varepsilon_{s1}^{p}\\ \varepsilon_{s2}^{p} - \varepsilon_{s1}^{p}\end{Bmatrix}_{2\times 1},\\ \bar{x}_s &= \begin{Bmatrix}\bar{x}_s^1\\ \bar{x}_s^2\end{Bmatrix}_{2\times 1}.\end{aligned} \tag{8}$$

Beside these linear inequality constraints, to ensure logical sequence of softening phase activation, the following nonlinear constraints must be considered:

$$\begin{aligned}&\bar{x}_s^1\left(-\bar{x}_s^1 - \bar{x}_s^2 + \varepsilon_s^{p} - \varepsilon_{s1}^{p}\right) = 0,\\&\bar{x}_s^2\left(\bar{x}_s^1 - \varepsilon_{s2}^{p} + \varepsilon_{s1}^{p}\right) = 0.\end{aligned} \tag{9}$$

Or, in compact form:

$$\bar{x}_s^{T} Z_s = \{0\}. \tag{10}$$

These complementarity conditions assure that $\bar{x}_s^1$ cannot assume a non-zero value before $\bar{x}_s^0$ reaches its limit value ε_{s1}^{p} and, in the same manner, $\bar{x}_s^2$ should remain zero until $\bar{x}_s^1$ become saturated, i.e., until it meets its limit value $\varepsilon_{s2}^{p} - \varepsilon_{s1}^{p}$. Finally for such a softening rule, the size of yield locus is related to the variable $\bar{x}_s^1$ using the following formula:

$$\alpha_s = 1 + h_s \bar{x}_s^1, \tag{11}$$

where h_s is a vector containing the softening coefficients h_s^j, i.e., the slope of middle part of softening rule depicted in Fig. 1c. It is necessary to emphasize again that the shape of yield locus is assumed to shrink uniformly, i.e., for all j yield planes, a unique h_s^j is assumed. However a non-homothetic change of the yield surface can be easily imposed by assuming different h_s^j for diverse yield planes. In this study, identical softening parameters are attributed to all yield modes to guarantee an isotropic evolution of the yield surface. Then, the yield criterion for section s can be written as follows:

$$Y_s = \mathbf{\Phi}_s^{T} f_s - \mathbf{H}_s \bar{x}_s - \{1\} \leqslant \{0\}. \tag{12}$$

In which $\mathbf{H}_s$ is a matrix with h_s vector in one column and zeros in second column.

2.2. Problem formulation

Nonlinear analysis procedures in general, try to satisfy equilibrium together with the yield constraints in Eq. (12). Various methods implement different approaches for the fulfillment of yield constraints. Some procedures solve the problem through the mathematical programming: in this case, the yield conditions are considered as the constraints in an optimization problem. Different researchers assume different objective functions for their optimization problem. In this study, the increment of dissipated energy has been taken as the function to be maximized.

In order to formulate the entire structural problem as a mathematical programming problem, all inequality constraints (i.e., yield and softening limits) will to be expressed at the global level using matrix notation. This is simply done by assembling the matrices obtained at local level. For instance, the yield conditions for all n candidate sections are collected and compacted in the following form:

$$Y = \mathbf{\Phi}^{T} f - \mathbf{H}\bar{x} - \{1\} \leqslant \{0\}. \tag{13}$$

In above formula, $\mathbf{\Phi}$ is the global yield matrix obtained by arranging $\mathbf{\Phi}_s$ matrices in block diagonal form. $\mathbf{H}$ is formed in the same manner, using $\mathbf{H}_s$ as block diagonal terms. f is the vector of generalized stresses vector, and finally, $\bar{x}$ is a vector of the softening variables for all sections.

The generalized stress vector f is decomposable into an "elastic" (f_s^{e}) and a "residual" (f_s^{p}) part. The elastic contribution is the result of a linear elastic analysis of frame under the current level of external actions. The residual term stands for the "relaxation effects" of plastic strains that may appear in critical sections. It is clear that both generalized stress parts (f_s^{e} and f_s^{p}) are only expressible at the global level. The first one can be computed using the global stiffness matrix and the external load vector, while the second one can be expressed by the global influence matrix $\mathbf{f}^{v}$, the global yield matrix $\mathbf{\Phi}$ and the plastic multiplier vector x. Accordingly, the generalized stress vector for the whole structure assumes the following form:

$$f = f^{e} + f^{p} = \lambda f^{0} + \mathbf{f}^{v}\mathbf{\Phi} x, \tag{14}$$

where λ is the load multiplier and f^0 is the internal force vector obtained as linear elastic response to external actions. Also, each column of the influence matrix, $\mathbf{f}^{v}$, represents the linear elastic structural response to a unit internal strain imposed at the corresponding section. It is worth noting that such analyses do not require any stiffness matrix assembly or inversion further to that already done for the initial linear elastic analysis of the structure. Replacing (14) into yield conditions (13) gives:

$$Y = \mathbf{\Phi}^{T}\mathbf{f}^{v}\mathbf{\Phi} x + \lambda\mathbf{\Phi}^{T} f^{0} - \mathbf{H}\bar{x} - \{1\} \leqslant \{0\}. \tag{15}$$

Considering $\{1\}^{T}\dot{x}$ as the objective function, with dots representing derivative with respect to ordering (not necessarily physical) time, the following Mathematical Programming (MP) problem can be defined:

$$\begin{cases}\max \quad \{1\}^{T}\dot{x},\\ \text{subject to}: \quad Y = \mathbf{\Phi}^{T}\mathbf{f}^{v}\mathbf{\Phi} x + \lambda\mathbf{\Phi}^{T} f^{0} - \mathbf{H}\bar{x} - \{1\} \leqslant \{0\},\\ \qquad\qquad Z = \mathbf{Q}x + \mathbf{W}\bar{x} - C \leqslant \{0\},\\ \qquad\qquad x^{T}Y = 0,\\ \qquad\qquad \bar{x}^{T}Z = 0,\\ \qquad\qquad x \geqslant 0,\\ \qquad\qquad \bar{x} \geqslant 0,\\ \qquad\qquad \bar{\lambda} \geqslant \lambda \geqslant 0,\\ \qquad\qquad \Delta \leqslant \bar{\Delta},\\ \qquad\qquad \theta \leqslant \bar{\theta}.\end{cases} \tag{16}$$

The last three constraints are added to put a limit on the load multiplier λ, sway/deflection, Δ, of some node(s), and effective generalized plastic strain, θ, in some section(s), respectively. As it will be discussed in the next section, this MP is usually solved at the beginning of each increment and because at each load step the plastic hinges resulted from the previous steps, cause some reduction in the remaining strength capacity of sections, the term {1} in yield constraints $Y \leqslant 0$ will be automatically modified at each load step. Similar to RBLP method, the nonlinear constraints will be satisfied implicitly during pivot finding in the Simplex table.

2.3. Plasticity events

When PWL constitutive models and fixed elastic parameters are used, as long as the proportionality of stress–strain does not change, the obtained response of structure to proportionally (or stepwise proportionally) varying external actions is theoretically exact, i.e., results are affected only by round-off errors not solution procedure (see e.g., [17,25]).

Accordingly, detection of the load levels for which this proportionality changes in any section is the key point toward non-holonomic analysis. Generally saying, "*unloading*" and "*reaching to yield surface corners*" in any active section are recognized as the cause of change in the aforementioned proportionality and, possibly, of divergence from exact responses in holonomic approaches.

Unloading happens when the state of stress in a section tends to leave a yield plane, which is mathematically equivalent to excluding the corresponding x variable from the set of active plastic multipliers. The latter situation happens when state of stress in some section tends to switch the yield plane (which is a special case of unloading) or stay at the corner (i.e., multiple yield plane activation in a section). Hereafter, these situations are referred to as *events* and in the occasion of any event the current Simplex table is *reset* and the solution is resumed in a *refreshed* Simplex table.

Resetting means recording the resulted values of the problem variables, available in the right hand side of corresponding active constraints of Simplex table, and replacing them by zero. This is mathematically equivalent to updating Y and Z constraints in the MP problem defined by Eq. (16) by using the following substitutions:

$$\begin{aligned} \lambda &= \hat{\lambda} + \dot{\lambda}, \\ \mathrm{x} &= \hat{\mathrm{x}} + \dot{\mathrm{x}}, \\ \bar{\mathrm{x}} &= \hat{\bar{\mathrm{x}}} + \dot{\bar{\mathrm{x}}}, \end{aligned} \tag{17}$$

where, the hatted variables refer to the accumulated values of variables from beginning up to the detected *event*, and dotted ones are the expected increments in the next loading stage. Obviously after resetting, the sign and complementarity constraints have to be hold for the increments of x and $\bar{\mathrm{x}}$. This physically means resuming the problem solution by assuming the accumulated internal forces and external load level as initial conditions for the rest of solution of the problem.

Refreshed Simplex table is the updated form of the Simplex table after performing the pivoting actions required for unloading a yield plane. Fortunately, refreshment does not impose any computational cost except three pivoting actions per each exiting plastic multiplier.

With reference to the aforementioned terms and definitions, the solution procedure is better illustrated in the next Section.

3. Solution procedure

The solution algorithm is comprehensively demonstrated in [21], but here it is discussed again in detail to outline the procedure of the proposed method for the case of softening. First of all, the Simplex table relevant to the initial (unstressed) configuration is shown in Table 1. In this table variables y, $\bar{y}$, ζ, δ, and ψ are slack variables corresponding to x, $\bar{x}$, λ, Δ, and θ respectively. Also the two parts of the simplex table in light and dark gray are referred to in the following as $\overline{\mathbf{D}}$ and $\overline{\overline{\mathbf{D}}}$, respectively. Since each row of the Simplex table corresponds to a yield plane, hereafter the variables x and y are addressed with only one subscript which refers to the row number where their corresponding "yield plane constraint" is placed in the simplex table.

The procedure followed for the solution of the Simplex problem is very similar to the RBLP method (for which some additional provisions is added to simplex method for considering complementarity conditions), but herein some additional cares have to be taken to detect any *events* defined in the previous Section. This procedure is better illustrated in the flowchart of Fig. 2, for which the description of each Step is mentioned hereunder.

Step 1. To start manipulation, it is noted that at the beginning all y variables are present in the set of Basic Variables (BV) and therefore, as a required by the complementarity constraints, none of x variables can enter the BV. Evidently, if the load multiplier λ remains zero no plastic hinge can form; therefore, the first variable that enters the BV is λ. At this time, according to the Simplex rules, a pivot row with minimum positive $b_j/\overline{\mathbf{D}}(j,i)$ ratio has to be determined for the exiting variable. Then the pivoting is made to enter λ into the corresponding pivot row. As a consequence, one of the slack variables, say y_k, leaves the BV and this means that the corresponding plastic multiplier, x_k, can now enter the BV set. In this way, always there exists a free plastic multiplier (FPM) ready to enter the BV set, but it must be selected in order to obtain the maximum gain in the objective function.

Table 1
Initial simplex table.

	$x_1^l \cdots x_1^m$	⋯	$x_n^l \cdots x_n^m$	$\bar{x}_1^1\ \bar{x}_1^2$	⋯	$\bar{x}_n^1\ \bar{x}_n^2$	λ	$y_1^l \cdots y_1^m$	⋯	$y_n^l \cdots y_n^m$	$\bar{y}_1^1\ \bar{y}_1^2$	⋯	$\bar{y}_n^1\ \bar{y}_n^2$	ζ	δ	ψ	b
y_1^l	* … *		* … *	* *		* *	*	1									1
⋮	⋮ ⋱ ⋮	…	⋮ ⋱ ⋮	⋮ ⋮	…	⋮ ⋮	⋮	⋱									⋮
y_1^m	* … *		* … *	* *		* *	*	1									1
⋮	⋮	⋱	⋮	⋮	⋱	⋮	⋮		⋱								⋮
y_n^l	* … *		* … *	* *		* *	*			1							1
⋮	⋮ ⋱ ⋮	…	⋮ ⋱ ⋮	⋮ ⋮	…	⋮ ⋮	⋮			⋱							⋮
y_n^m	* … *		* … *	* *		* *	*			1							1
$\bar{y}_1^l$	* … *		* … *	* *		* *	0				1						0
$\bar{y}_1^2$	* … *	…	* … *	* *	…	* *	0				1						0
⋮	⋮	⋱	⋮	⋮	⋱	⋮	⋮					⋱					⋮
$\bar{y}_n^l$	* … *		* … *	* *		* *	0						1				0
$\bar{y}_n^2$	* … *	…	* … *	* *	…	* *	0						1				0
ζ	* … *	…	* … *	* *	…	* *	*							1			$\bar{\lambda}$
δ	* … *	…	* … *	* *	…	* *	*								1		$\bar{\Delta}$
ψ	* … *	…	* … *	* *	…	* *	*									1	$\bar{\theta}$
Cost	−1 ⋯ −1	…	−1 ⋯ −1	0 0	…	0 0	0	0 ⋯ 0	…	0 ⋯ 0	0 0	…	0 0	0	0		0

Step 2. As a Simplex rule, the variable that enters the BV set is the one with the most negative cost coefficient ($COST_{min}$) and it can be either the FPM or one of the previously expelled-out slack variables.

Step 3. If, according to the most negative cost criterion, a slack variable is selected for entering the BV set, it is a sign of unloading. In this situation more investigation is required to see if the corresponding plastic multiplier will immediately return to the BV or not. In such cases, the algorithm jumps to Step9, otherwise it continues through Step4.

Step 4. When the cost coefficient associated to a FPM becomes the most negative coefficient, another yield surface is becoming active. According to the Simplex rules, the FPM (x_i) must be inserted in the row j, which results in the smallest non-negative ratio $b_j/\overline{\mathbf{D}}(j,i)$. Physical interpretation of such selection lies on positiveness of plastic multiplier increments. If a row is excluded from the $b_j/\overline{\mathbf{D}}(j,i)$-check, it may result in a negative increment (decrease) of its corresponding basic variable. In the proposed algorithm this lemma was used, and the row corresponding to λ was intentionally excluded from the pivot row-check. This led to automatically admitting the negative load multiplier increments addressed in [15] for softening problems. Also if there exist more than one free row with the same smallest ratios, it mathematically means that there are "multiple stationary points" it can be physically interpreted as "possible bifurcation in the solution". Such cases can also appear due to initiation of simultaneous plasticity in some sections, as it may happen in symmetric frames, which is not really a case of instability. Fortunately, such cases can be easily managed by selecting one row for pivoting and investigating the chance of other row(s) to be selected as pivot row in the next subsequent pivot search(s). If this assessment determines no chance for the remaining rows to become pivot row immediately, the case is bifurcation.

Step 5. It may happen that the selected pivot row is already occupied by another plastic multiplier. If this is the case, the existing plastic multiplier (that is called "obstacle" plastic multiplier (OPM)) should be replaced by FPM, i.e., the OPM should be unloaded in order to prepare ground for entering the FPM. Otherwise, the solution procedure must be followed form the next Step.

Step 6. If a FPM belongs to a joint for which another yield plane is already active, it means that two yield planes will be simultaneously active. At this stage another restriction, (not considered in holonomic approaches), will be considered. This case is recognized as "*staying on corner*", and the algorithm jumps to Step 12. Otherwise the process is followed from Step 7.

Step 7. If the FPM is the first one activated in the joint, it can enter the BV set and the pivoting is made around $\overline{\mathbf{D}}(j,i)$, in order to enter the FPM into the selected pivot row j. This pivoting action will produce changes in problem variables, i.e., plastic and load multipliers, and the loading process will continue.

Step 8. As it was mentioned in Step5, it can happen that the selected pivot row contains an obstacle plastic multiplier (OPM), which prevents the entry of the FPM into the BV set. This is a trivial case of unloading and it is one of the *events* introduced above. In such cases, the OPM is forced to exit after *resetting*.

Step 9. If $COST_{min}$ corresponds to a slack variable, say y_j, as was stated in Step3, some checks are needed for making the right decision. In order to bring back a previously expelled slack variable y_j into the BV set, the complementarity condition requires that, the corresponding plastic multiplier x_j (hereafter SPM) exits from the BV set. On the other hand, and after unloading (if it is the case), the algorithm will continue with entering the FPM into the BV set. Suppose that FPM is x_i. It may happens that the row corresponding to the exited SPM be selected as the pivot row. If this happens, SPM will return into BV immediately after exit and the performed pivot actions impose some vain computational costs on the analysis. To avoid such situations, it is only sufficient to consider the sign of some index ratio r defined as follows:

$$r = \overline{\mathbf{D}}(j,i)/\overline{\overline{\mathbf{D}}}(j,j). \tag{18}$$

In fact the calculated index ratio r is the value that will appear in the cell (j,i) of $\bar{\mathbf{D}}$ matrix after performing required refreshments toward exiting SPM. A negative index ratio r guarantees that row j will not be selected during the next pivot row search and SPM has to be expelled out. In the case of positive index ratio r, variables corresponding to the next minima in cost row have to be verified.

Step 10. If SPM shows immediate return tendency, we should consider the next $COST_{min}$, i.e., 2^{nd}, 3^{rd}, ... minima in the cost row. This loop is repeated until a slack variable fulfills the entering criteria (as described in Step9) or FPM obtains the most negative cost among the remaining shadow cost coefficients.

Step 11. If $r < 0$, an unloading will happen. Therefore the process of unloading can be followed after *resetting*. It is worth noting that it is possible to have simultaneous unloading in several sections until a FPM becomes qualified for entering into the BV set. In such cases, as it is seen in the flowchart, a series of unloadings will happen through the Steps 2-3-10-12-2. The interesting point is that because of *resetting*, there will be no changes in variable values, i.e. load and plastic multiplier increments remain zero until the FPM enters the BV set.

Step 12. If the FPM belongs to an active joint and is qualified for entering into the BV set, the case is "*staying on corner*". In this case before entering the FPM into the BV set only a *resetting* is needed.

What should be added to the above explanations is that in the case of any local unloading (i.e., exiting any plastic multiplier from BV set), all section variables including plastic multipliers and corresponding softening variables have to exit in sequence.

In the case of reaching a termination criterion, i.e., maximum load, target sway/deflection, allowable equivalent plastic strain in some section, etc., the corresponding row will be selected as pivot row and after pivoting no FPM will be found to continue the process and the algorithm will stop.

It should be underlined that a reduced storage memory and less computational effort will be spent if the Revised Simplex method [26] in parallel to the above provisions is employed. For instance, instead of building and storing the whole $\overline{\mathbf{D}}$ matrix, a selected column of $\overline{\mathbf{D}}$ will be computed by simple algebraic manipulation. Details on the implementation of such techniques are out of scope of this paper.

4. Illustrative examples

In order to numerically validate the proposed algorithm, two series of examples are selected from the literature.

The first set of frames, presented in part (A), are taken from [17] in which a step-by-step solution scheme is employed for the anal-

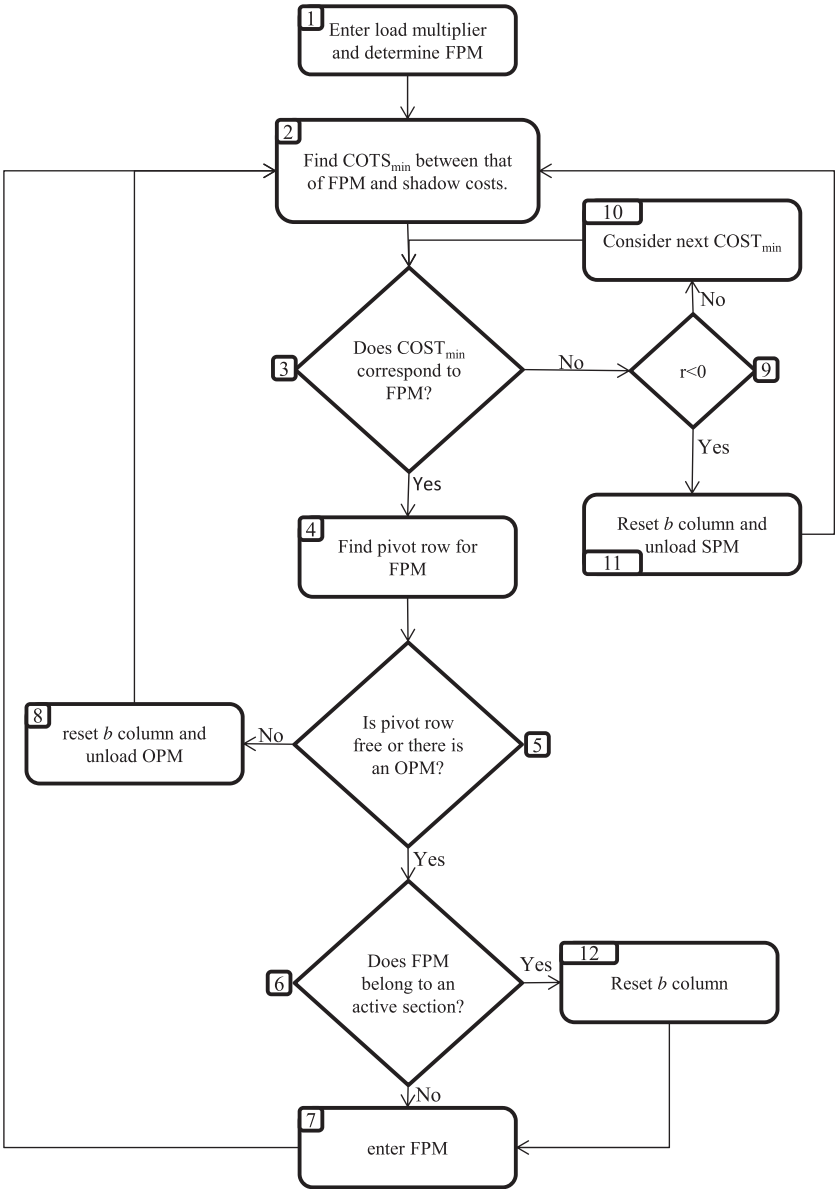

Fig. 2. Solution flowchart.

ysis. These examples are considered to show ability of the proposed method in returning the exact responses of structures.

The second set of examples, presented in part (B), are selected from [20], where a holonomic approach has been adopted to find the solutions. The aim of presenting these examples is not to compare the results, because the response of the proposed method is non-holonomic and there is no point to be compared with holonomic results. However, these examples are considered here to show the ability and capability of the proposed method in solving large-scale problems and also to demonstrate its efficiency in terms of computing time.

All analyses have been performed on a laptop (*msi* GE620, Intel Core i7-2630QM with 8-GB RAM and Win7 operating system) using a code developed in MATLAB environment.

4.1. Part A

For the frame considered in [17], pure flexural plastic hinges (with no interaction between axial force and bending moment) are attributed to the critical sections. It is obvious that, for this example, the developed formulation has to be slightly modified: this is simply done by eliminating the axial force and its corresponding yield planes and variables in the problem formulation. This frame is solved for several softening rates and the exact solutions are determined: in spite of its very ordinary layout, relatively complicated responses are observed.

4.1.1. Example A1: Single bay, single story bending frame

The single-bay single-story frame shown in Fig. 3, with the height of 3 m, span length of 4 m and F = 100 kN, is considered as the first example. Mechanical properties of the frame members and sections are given in Tables 2 and 3 respectively. The softening evolution law shown in Fig. 1c is assumed for the Sections 1–5, except that the ultimate strength is set to zero. An effective plastic strain ratio $\vartheta = \varepsilon^{p}_{s2}/\varepsilon^{p}_{s1}$ is defined and used to define the softening rates in diverse analysis cases. As shown, the frame is loaded with proportionally increasing lateral and gravity point loads and the task is to determine response of the structure and corresponding

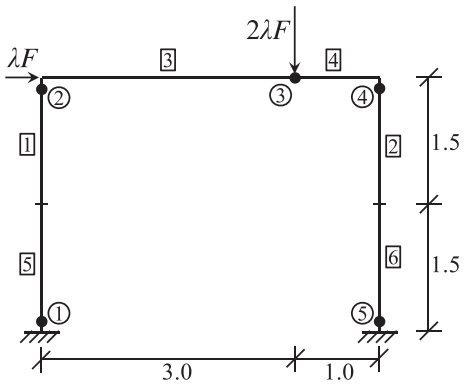

Fig. 3. Single bay, single story bending frame of example A1 [17].

Table 2
Mechanical properties of members of the frame of example A1.

Flexural stiffness (MN m^2)	Axial stiffness (MN)	Element
33.99	1953	1, 2
79.31	2740	3, 4, 5, 6

Table 3
Mechanical properties of sections of the frame of example A1.

ε^p_{s1}	α_{min}	Bending limit load (kN m)	Section
1.362e−3	0	236.8	1, 5
9.103e−4	0	420.7	2, 3, 4

collapse/ultimate loads for effective generalized plastic strain ratios ϑ=∞, 100, 15 and 5. To capture any collapse and limit the analysis results to small deformation regime, the horizontal sway at node no. 2 is limited to Δ =18 mm. Reaching intensive plastic deformation in frame sections ($\varepsilon^p = 10\varepsilon^p_{s2}$) or appearing bifurcation in the response of the structure, are also considered as conditions of analysis termination.

Results: Formulating the problem and starting load application indicates plasticity initiation in Section 4 at the load level λ=2.4175 for all softening rates. The peak loads corresponding to diverse softening rates $\vartheta = \infty$, 100, 15 and 5 have been found to be 3.8571, 3.7645, 3.2249 and 2.6679, respectively. The load displacement history of the monitored joint no. 2 and the sequence of emerged hinges are visualized in Fig. 4. The bifurcation addressed in [15] for the analysis case $\vartheta = 5$ was detected correctly by the proposed algorithm. In that case and at the load level λ=2.6458 (indicated by *e* in Fig. 4d) and during pivot row search two free rows with the same nonzero minimum ratios are found and accordingly two different plastic strain vector paths were determined: one having the Section 3 unloaded and further plastic deformations in Section 4, and the other one with plastic deformations in both Sections 3 and 4.

The resulted responses and plasticity history exactly coincide with those reported in [17], but the proposed algorithm had the following advantages compared to the step by step algorithm.

- Load levels for which a new plastic hinge forms or any plasticity event tends to occur are captured automatically.
- Plastic strain directions for initiating new load step were simply determined following the proposed maximization criterion. No sub-problem was formed and solved for getting directions in plastic strain space.
- Negative load increments were automatically captured during the solution process.

4.2. Part B

For all frames considered in this part, material constitutive model is considered to be a 6-mode PWL yield surface, like that of Fig. 1a, with $\bar{N}_0 = 0.15$. To conform with assumptions of the reference [20], it is assumed that softening initiates from the earliest plasticity stage, i.e., $\varepsilon^p_{s1} = 0$, and the absolute flexural component of plastic deformation in each section is considered as effective plastic strain. This is simply applicable to the proposed formulation by attributing the absolute of values appearing in the second row of yield matrix $\mathbf{\Phi}_s$ into $\bar{\mathbf{Q}}_s$:

$$\bar{\mathbf{Q}}_s = abs([\,\varphi^s_{21} \quad \varphi^s_{22} \quad \varphi^s_{23} \quad \varphi^s_{24} \quad \varphi^s_{25} \quad \varphi^s_{26}\,]). \tag{19}$$

For all frames, the analysis is performed for two cases; (*a*) accounting for interaction of axial force and bending moment, and (*b*) considering only pure flexural plasticity. It is obvious that for case (*b*) some modifications have to be made to the formulation as it was done for part (A). In addition, in order to better understand and visualize the reduction of load carrying capacity due to softening behavior, the elastic-perfectly-plastic responses of the frames have been also taken from [21]. To capture any probable collapse and limiting analysis and results into small deformations regime, the horizontal sway at the topmost story is restricted to $\bar{\Delta} = 0.75$ m for all examples. All frames are made of steel, for which the Young modulus is assumed to be E = 200 GPa.

4.2.1. Example B1: Single bay, three story dual frame

Fig. 5 demonstrates the layout of a single bay, three story steel frame with eccentric bracings. Geometrical and mechanical properties of the frame sections are listed in Table 4.

For this frame, it is assumed that the bracing members act in perfect plasticity. The aim is to load the structure and determine the exact structural responses using the proposed algorithm.

Results: By formulating the problem in case (*a*) and applying the external loads, it is seen that the first plastic hinge appears at the load level λ = 57.8529 in a beam section, which is the same for the case (*b*). At λ = 67.3990, the state of internal force in section A reaches a corner and tends to change the yield mode. Refreshing the Simplex table and continuing the solution process shows that at the load level λ = 67.4330 the state of internal force in section B tends to change the yield plane. Afterwards, when the horizontal deflection at topmost story is 0.4114 m, the peak load level λ = 117.5294 is reached and after this point the decreasing branch of response starts with a variety of events. For instance at the load level λ = 117.1152 the section C reaches a corner and tends to stay on it. The loading process can continue up to the load level λ = 112.6912, for which the sway at the top story reaches its limit value 0.75 m and the procedure stops. In the reference [20], for the holonomic analysis of this example, the peak load and its corresponding deflection are reported to be 117.617 and 0.382 m respectively.

In case (*b*), the solution process reaches to the peak load λ = 119.8446 without any specific event at the horizontal deflection of 0.3957 m. Continuing with the analysis, the sway limit of 0.75 m is reached for a load level of 114.0656 and the procedure stops at this stage. The same peak load (119.845) is reported in [16] for this case, which is exact as a result of "no events".

The history of topmost story sway for the cases (*a*) and (*b*) are depicted together in Fig. 6a, beside the elastic-perfectly-plastic response of the structure. As expected, it is seen that considering softening for frame sections in case (*a*) a load bearing reduction of about 4% is obtained with respect to perfect plasticity. Moreover, the layout of the plastic hinges at the peak load is shown in Fig. 6b, in full agreement with that reported in [20].

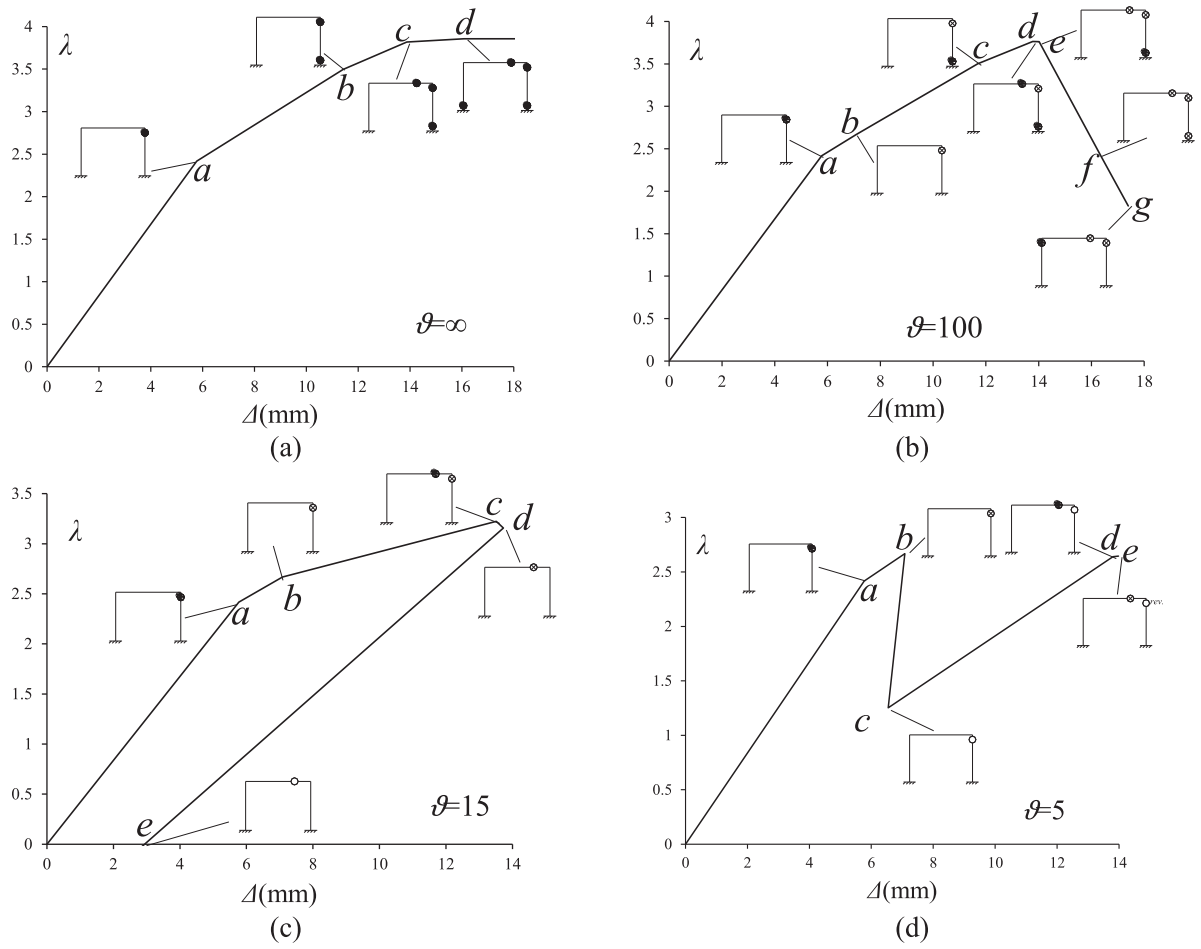

Fig. 4. Load multiplier (λ) versus horizontal displacement of the joint no. 2 (Δ) resulted in example A1 for different softening rates $\vartheta=\infty$, 100, 15 and 5. Diverse plasticity stages of sections are separated by ●, ⊗, and ○ which are corresponding to $0 < \varepsilon^p < \varepsilon^p_{s1}$, $\varepsilon^p_{s1} < \varepsilon^p < \varepsilon^p_{s2}$, and $\varepsilon^p > \varepsilon^p_{s2}$ respectively.

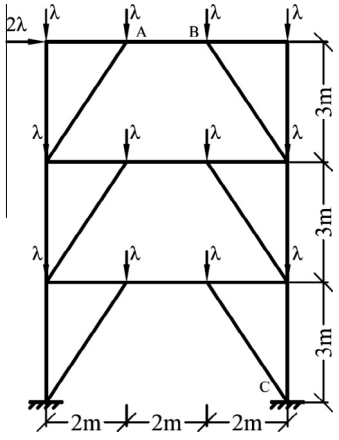

Fig. 5. Single bay, three story dual frame of example B1, [20].

Table 4
Geometric and mechanical properties of members for the frame of example B1.

ε^p_{s1}	ε^p_{s1}	α_{min}	M_p (kN m)	N_p (kN)	Cross section	Element
0.8119	0	0.7	548.8	4200	310UC118	Column
0.4211	0	0.7	57.6	742.4	200UB18.2	Beam
–	–	–	57.75	1365	SHS125/125/9	Bracing

The CPU time allocated for analysis via the proposed algorithm was 0.10 second for combined bending and axial with softening, 0.04 second for pure flexural with softening, and 0.04 second for perfect plasticity [21].

4.2.2. Example B2: Three bay, three story dual frame

Fig. 7 shows the layout of a three bay, three story steel frame reinforced by the means of eccentric bracings. Geometrical and mechanical properties of the frame sections are listed in Table 5.

In this example, some constant 50 kN dead loads are applied to the structure prior to gradually applying lateral forces. It is easily verified that the set of gravity loads does not cause any yield or plasticity initiation in the frame. Accordingly the effects of dead loads are simply imposed to the solution by deducing the corresponding internal forces from the initial strengths of frame sections. Here again the bracing members are supposed to behave in an elastic-perfectly plastic way and the task is to load the structure and determine the exact responses using the proposed algorithm.

Results: By formulating the problem and applying the loads it is observed that the plasticity starts at load level $\lambda = 59.0592$ at a beam section in both analysis cases (a) and (b). By following the solution procedure in case (a) it is found that at the load level $\lambda = 81.1082$, when frame experienced plasticity in 12 critical sections, internal force state in beam section A reaches to a corner and tends to switch the yield mode. The same event takes place for the beam section B at load level $\lambda = 81.1671$. After that, many events occur over the critical frame sections to reach maximum load level $\lambda = 116.6696$ and its corresponding sway 0.2814 m.

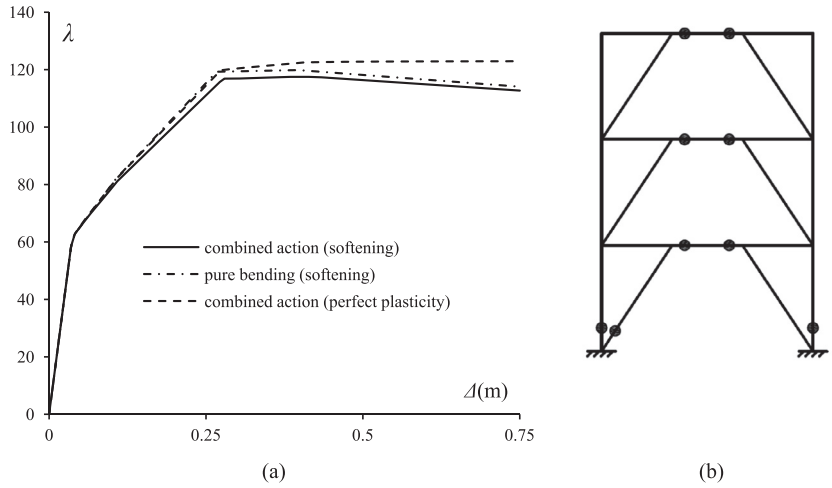

Fig. 6. (a) Top story sway, (b) final layout of the plastic hinges for both analysis cases *a* and *b* in the dual frame of example B1.

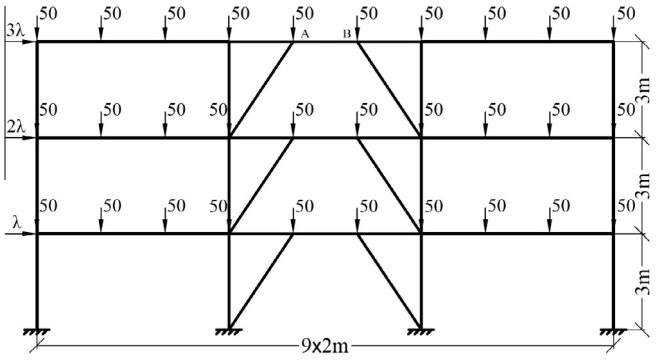

Fig. 7. Three bay, three story dual frame of example B2 [20].

Solution can be followed in descending branch to reach the limit sway 0.75 m at load level $\lambda = 110.3997$. In this example, by considering the softening behavior for frame sections the load bearing capacity is reduced by an amount of 3%. For this analysis case, in Ref. [20], $\lambda = 116.785$ and $\Delta = 0.280$ m are reported as the peak load and its corresponding sway respectively.

By reformulating the frame and following the solution process in pure flexural plasticity, case (*b*), it is seen that the structure experiences no event and the peak load of frame is found to be $\lambda = 118.9824$, with a 0.2696 m sway. The analysis follows the softening branch and stops at the load level $\lambda = 111.4063$, at which the sway limit 0.75m is reached. Since no specific events were detected in this analysis case, proportionality holds during the loading phase up to the peak load and even a holonomic approach can re-

Table 5
Mechanical properties of members of the frame of example B2.

ε^p_{s1}	ε^p_{s1}	α_{min}	M_p (kN m)	N_p (kN)	Cross section	Element
0.8119	0	0.7	548.8	4200	310UC118	Column
0.4432	0	0.7	102.08	1046.4	250UB25.7	Beam
0.8864	0	0.7	102.08	1046.4	250UB25.7	Beam (outer bays at point loads)
–	–	–	80	1235.2	150UC30	Bracing

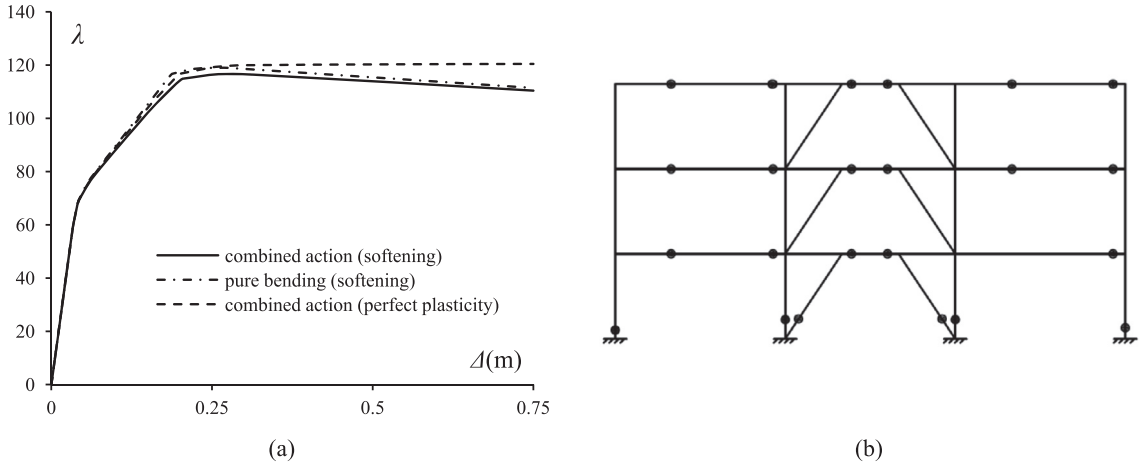

Fig. 8. (a) Top story sway, (b) final layout of the plastic hinges for the both analysis cases *a* and *b* in the dual frame of example B2.

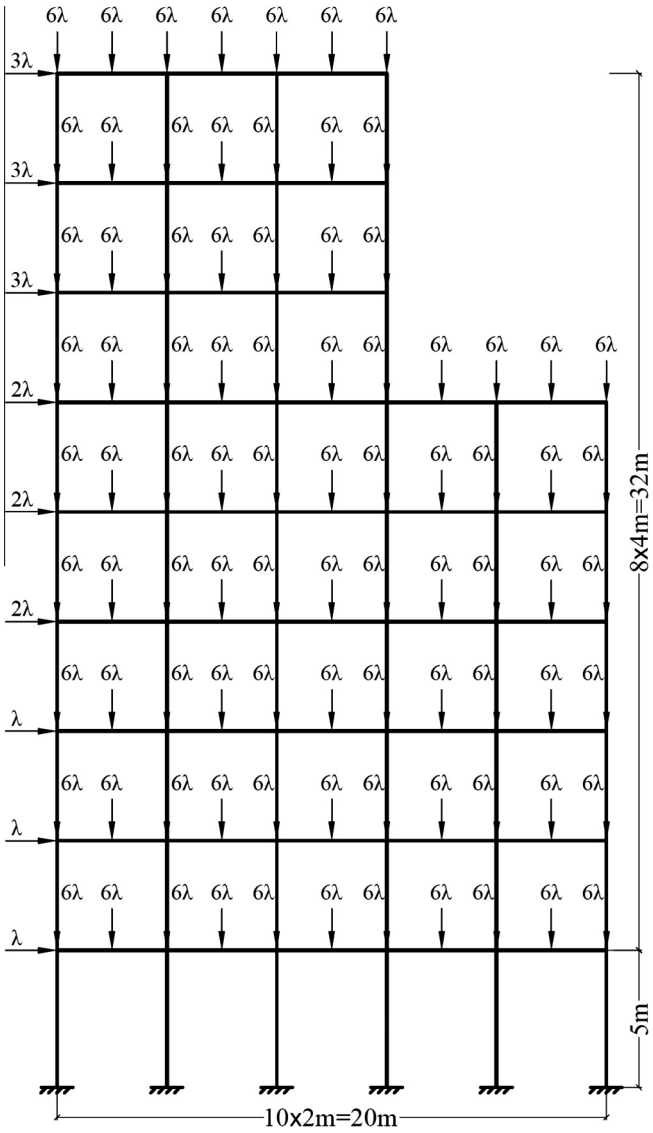

Fig. 9. Multistory bending frame of example B3 [20].

Table 6
Mechanical properties of members of the frame of example B3.

ε^p_{s1}	ε^p_{s1}	α_{min}	M_p (kN m)	N_p (kN)	Cross section	Element
0.0324	0	0.7	1988	11704	400WC328	Column
0.0341	0	0.7	552	3150	460UB82.1	Beam

turn the exact solution. As it can be seen, the same peak load level $\lambda = 118.982$ is reported in [20].

History of top story sway and layout of the plastic hinges, corresponding to the peak load in both cases (*a*) and (*b*), are shown in Fig. 8. Here, again, the plastic joints distribution at peak load coincides with that reported in [16]. The CPU time used for the analyses of this example via the proposed algorithm was 0.92 second for combined bending and axial with softening, 0.19 second for pure flexural with softening, and 0.38 second for perfect plasticity[21].

4.2.3. Example B3: Multistory bending frame

The last example presented here is the multi-story bending frame of Fig. 9. Increasing gravity and lateral loads are applied to the structure proportionally, as shown in the same Figure. Geometrical and mechanical properties of frame sections are given in Table 6.

Results: By formulating the problem and following the outlined procedure, it is seen that the first plastic hinge appears at the load level $\lambda = 55.3585$ in both cases (*a*) and (*b*). In case (*a*), the solution process gives the peak load level $\lambda = 79.7090$ at the sway 0.3297 m, with 44 active joints. Thereafter, local unloading starts to take place at some sections immediately, and the descending branch of the load–displacement curve follows. After several events in plastic joints, sway limit 0.75 m is reached at the load level $\lambda = 72.7397$. The same peak load and corresponding sway are reported in [20].

Reformulating the frame in pure flexural plasticity mode, case (*b*), the peak load turns out to be $\lambda = 88.0272$, and the corresponding sway 0.3501 m. After this, the frame response shows the descending branch and, finally, at the load level $\lambda = 85.2084$ the solution terminates due to reaching the limit of the frame sway. For this case, a peak load $\lambda = 88.622$ is reported in [20], whereas exact solution of $\lambda = 88.0272$ was expected in this case because of no detected events.

The history of top story sway is plotted in Fig. 10a. Also the layouts of active plastic hinges, corresponding to the peak loads

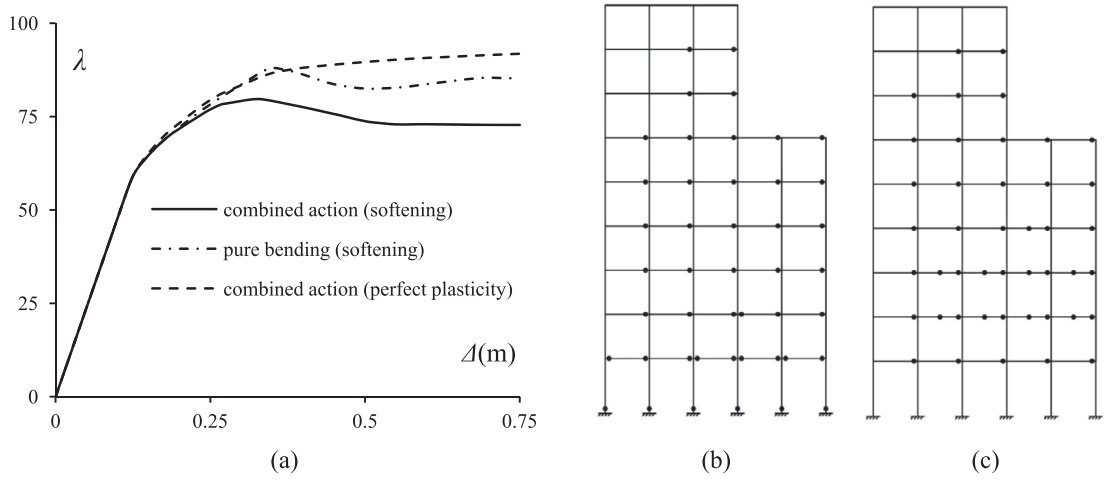

Fig. 10. (a) Top story sway, (b) final layout of the plastic hinges for analysis case *a*, and (c) final layout of the plastic hinges for analysis case *b* in the bending frame of example B3.

determined in analysis cases (*a*) and (*b*) are shown in Fig. 10b and c, respectively. The plastic joint scheme for case (*a*) coincides with the layout reported in [20], but the other one is slightly different.

The analysis, in these examples, required 14.91, 9.77 and 6.5 seconds of CPU time for a) combined bending and axial force with softening, b) pure flexural with softening and c) perfect plasticity [21], respectively.

5. Conclusions

In this paper, a new algorithm for the nonlinear analysis of softening frames is proposed. The algorithm is an extension of the previously proposed "dissipated energy maximization" (DEM) approach, for the analysis of elastic–plastic frames by the authors (see [21]). The basis of the formulation is the piecewise linear elasto-plastic constitutive models for the critical-sections. The problem of gradual development of plastic hinges in the structure is given a mathematical programming formulation and solved. The results of this research can be summarized as follows:

(a) In the proposed algorithm, exactness and stability features of the step-by-step solution scheme are preserved, i.e., except the errors arising from the piecewise linear approximation of the yield locus and from the unavoidable numerical round-off errors, the results are theoretically free of errors. Also since the formulation is a reflection of the behavior of structure, as long as the structure is stable under the applied loads, the solution procedure is stable.
(b) The proposed maximization criterion was found to serve as a quite efficient and reliable objective function in formulating the optimization problem of softening frames. Using this criterion, the algorithm became capable of detecting the unloadings as well as reaching a corner in the yield locus in the space of plastic multipliers and intelligent in finding the exact pass of nonlinear behavior of the structure.
(c) Comparison of CPU times used for Examples B1, B2 and B3 with the other methods in the field, clearly shows the superiority and efficiency of the proposed method
(d) Instead of applying the negative load increment solution suggested by [17], in the proposed algorithm any descending branch and elastic unloading is captured and handled automatically.
(e) The algorithm can recognize the solution bifurcations due to softening.

The examples show that the proposed algorithm is robust, versatile and efficient in the nonlinear analysis of framed structures, with or without softening.

References

[1] Bažant ZP. Scaling of failure of beams, frames and plates with softening hinges. Meccanica 2001;36:67–77.
[2] Jirasek M, Bazant ZP. Inelastic analysis of structures. Chichester, UK: Wiley; 2002.
[3] Crisfield MA. Non-linear finite element analysis of solids and structures, Volume 1: Essentials. John Wiley & Sons, Baffins Lane, Chichester, West Sussex PO19 IUD, England, 1997.
[4] Crisfield MA. Non-linear finite element analysis of solids and structures, Volume 2: Advanced Topics. John Wiley & Sons, Baffins Lane, Chichester, West Sussex PO19 IUD, England, 1997.
[5] Zienkiewicz OC, Taylor RL. The finite element method. 5th ed. Oxford: Butterworth-Heinemann; 2000.
[6] Cohn MZ, Maier G, Grierson DE. Engineering plasticity by mathematical programming. New York: Pergamon Press; 1979.
[7] Hill R. The mathematical theory of plasticity. Oxford, UK: Oxford University Press; 1950.
[8] Greenberg HJ, Prager W. Limit design of beams and frames. Proc ASCE 1951;77:1–12.
[9] Maier G, Grierson DE, Best MJ. Mathematical programming methods for deformation analysis at plastic collapse. Comput Struct 1977;9:599–612.
[10] Maier G. A quadratic programming approach for certain classes of non-linear structural problems. Meccanica 1968;3:121–30.
[11] Maier G. Quadratic programming and theory of elastic-perfectly plastic structures. Meccanica 1968;3:265–73.
[12] Maier G. A matrix structural theory of piecewise-linear plasticity with interacting yield planes. Meccanica 1970;5:55–66.
[13] Cottle RW, Pang JS, Stone RE. The linear complementarity problem. San Diego: Academic Press; 1992.
[14] Maier G, Giacomini S, Paterlini F. Combined elastoplastic and limit analysis via restricted basis linear programming. Comput Method Appl Mech Eng 1978;19:21–48.
[15] Maier G, Carvelli V, Cocchetti G. On direct methods for shakedown and limit analysis. Eur J Mech A/Solids 2000;19:S79–S100.
[16] Giambanco F. Elastic plastic analysis by the asymptotic pivoting method. Comput Struct 1999;71:215–38.
[17] Cocchetti G, Maier G. Elastic–plastic and limit-state analyses of frames with softening plastic-hinge models by mathematical programming. Int J Solids Struct 2003;40:7219–44.
[18] Lógó J, Taylor JE. Analysis of elastic-softening structures using a mixed extremum principle. In: Proceedings of NATO/DFG ASI, Berchtesgaden, Sept 23–Oct 4, 1991;3:286–93.
[19] Kaliszky S, Lógó J. Mixed extremum principles for the analysis of trusses with bilinear force-deformation characteristics. Mech Struct Mach: Int J 1994;22(4):429–56.
[20] Tangaramvong S, Tin-Loi F. Simultaneous ultimate load and deformation analysis of strain softening frames under combined stresses. Eng Struct 2008;30:664–74.
[21] Mahini MR, Moharrami H, Cocchetti G. A dissipated energy maximization approach to elastic-perfectly plastic analysis of planar frames. Arch Mech 2013;65(3):171–94.
[22] Kaliszky S, Lógó J, Merczel DB. Softening and hardening constitutive models and their application to the analysis of bar structures. Mech Des Struct Mach: Int J 2011;39(3):334–45.
[23] Maier G. Piecewise linearization of yield criteria in structural plasticity. Solid Mech Arch 1976;2:239–81.
[24] Tin-Loi F. A yield surface linearization procedure in limit analysis. Mech Struct Mach 1990;18:135–49.
[25] König JA. On exactness of the kinematical approach in the structural shakedown and limit analysis. Ing Arch 1982;52:421–8.
[26] Gass SI. Linear programming methods and applications. 4th ed. New York, NY: McGraw-Hill; 1975.